Etch Pits in Heliodor and Green Beryl From the Volyn Pegmatites, Northwest Ukraine: A Diagnostic Feature

Gerhard Franz, Oleksii A. Vyshnevskyi, Volodymyr M. Khomenko, Peter Lyckberg, and Ulrich Gernert

Green beryl and the yellow beryl variety heliodor are well known from the Volyn pegmatite field in Ukraine, and this study presents details of their morphological characteristics. Visible etch pits are characteristic of beryl from this locality. In addition, they may contain an organic matter called kerite. Formation of the etch pits is associated with a fluorine-rich, late-stage fluid phase. Etch pits on the pinacoidal face have a hexagonal outline and a pointed bottom (originating at linear defects) transitioning to etch pits with very steep walls, and they occur in three different orders of magnitude: ≤500 µm, ≤50 µm, and 1–3 µm. On the first-order prismatic faces, etch pits with a flat bottom (originating from point defects) or pointed bottom are square to rectangular, the latter oriented parallel or perpendicular to the beryl's *c*-axis. Flat bottom etch pits are more abundant than pointed bottom and also occur in three different orders of magnitude. In addition, small etch pits with a canoe shape and porosity on the nanometer scale were observed. Scanning electron microscopy of these etch pits was used to distinguish uncut stones from other pegmatitic beryls, but these phenomena are also visible with an optical microscope or even with a loupe.

Paleoproterozoic pegmatites near Khoroshiv (formerly Volodarsk-Volynskyi) in northwest Ukraine are known as a source of high-quality green beryl and the yellow beryl variety heliodor (e.g., Koshil et al., 1991; Simmons, 2014, and references therein). The green beryl's color can be very intense but never reaches the typical emerald color. Aquamarine is also claimed from the Volyn pegmatite field, but very rarely, and emerald from southeast Ukraine (Franz et al., 2020) is the country's only other important gem beryl occurrence. The finest specimens of Volyn beryl with color between green and yellow (figure 1) and size of up to 140 cm in length are displayed in the Museum of Precious and Decorative Stones in Khoroshiv (Vasylyshyn et al., 2001), while gem-quality crystals up to 55 cm have been sold abroad.

Since 1931, the pegmatites have been mined extensively for piezo quartz, which occurs in exceptionally large crystals from one to two meters (Lyckberg, 2005; Lyckberg et al., 2009, 2019). In addition to beryl, which is present in ~2% of the pegmatites, approximately 10% of these pegmatites contain gem-quality topaz. Among the first gem findings was topaz in 1931–1933, and later gem beryl was recovered as a byproduct.

In Brief

- Gem-quality crystals of green beryl and heliodor from the Volyn pegmatite field in Ukraine show spectacular dissolution features.
- Etch pits resulting from the dissolution are rectangular on prismatic faces and hexagonal on pinacoidal faces.
- The etch pits occur in different sizes and overlap each other, indicating different stages of dissolution that are diagnostic for uncut stones.
- Fossil organic matter known as kerite can be attached to the beryl crystals.

Mining for heliodor continued after World War II, but this material was only available in Eastern Europe. The first crystals reached the Western European market in 1980, and in 1987 Volyn beryl finally emerged

See end of article for About the Authors and Acknowledgments.
Gems & Gemology, Vol. 59, No. 3, pp. 324–339,
http://dx.doi.org/10.5741/GEMS.59.3.324

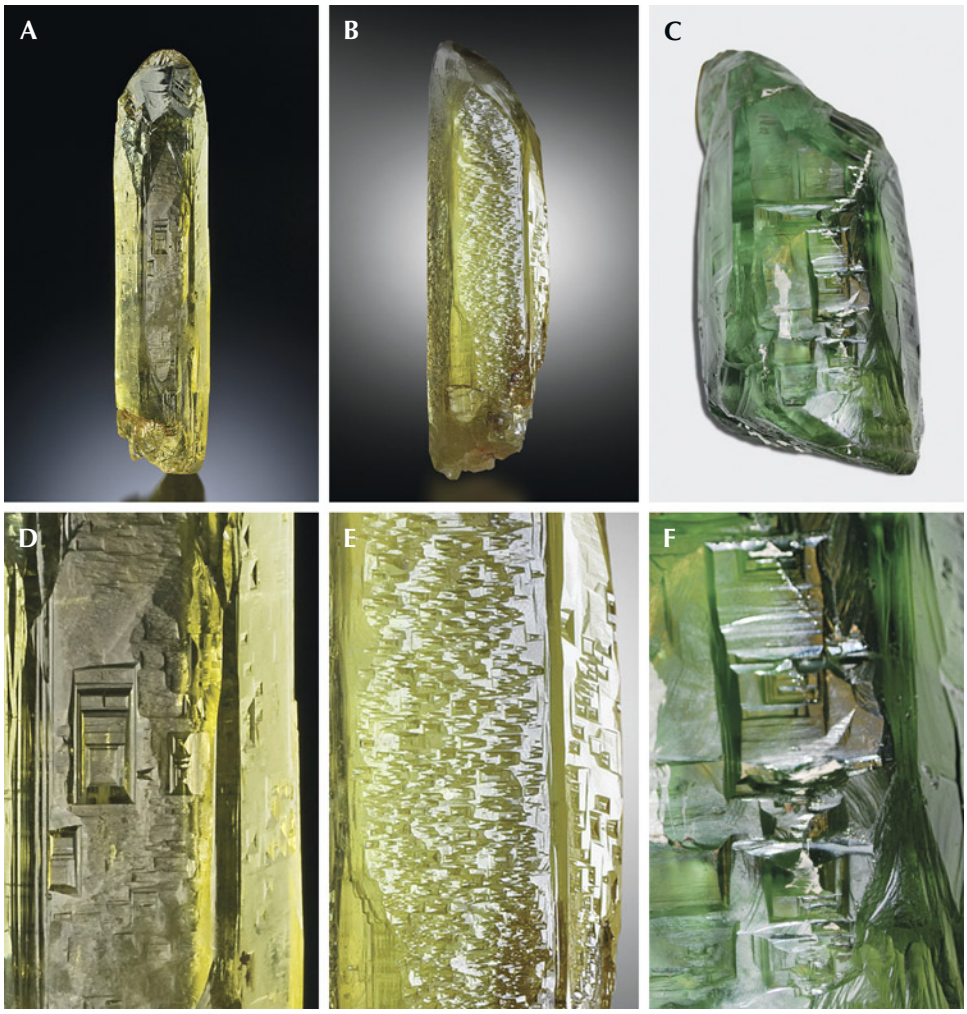

Figure 1. Yellowish green heliodor and green beryl from Volyn, oriented with the c*-axis vertical (top row) and detail views of the prismatic faces (bottom row). A and D: An 8.5 cm crystal with well-developed prismatic faces and strongly sculptured end faces; the detail view shows F-type etch pits elongated parallel to the* c*-axis. B and E: Transition from prismatic face (1.8 cm wide) to sculptured pyramidal face with triangular hillocks (compare with the SEM image in figure 10); the detail view shows dominantly asymmetrical P-type etch pits. C and F: A 2.683 kg deep green crystal measuring 18 × 10 × 9 cm with rectangular F-type etch pits, mostly oriented perpendicular to the* c*-axis. The samples in A and B are from the collection of Peter Lyckberg. The sample in C, named "Professor Pavlyshyn," is from the Museum of Precious and Decorative Stones in Khoroshiv. Photos by Peter Lyckberg (A and B) and Gerhard Franz (C).*

at the gem shows in Tucson. Many of these were used for cutting (figure 2), but a large number of fine mineral specimens were also preserved.

Since the early 1990s, the Volyn Quartz Samotsvety Company has conducted mining for beryl and topaz. Lyckberg et al. (2009) reviewed the mining and collecting history, the geology, and the formation of chambers within the pegmatites. That article also contains a list of accompanying minerals in the pegmatite and several photos showing the etch pits.

A characteristic feature of Volyn beryl crystals is their morphology, with exceptionally large dissolution features (etch pits), described on the basis of light microscopy by Bartoshinskiy et al. (1969) and Lazarenko et al. (1973). The prism faces show rectangular cavities with negative crystal faces, while the basal planes show negative, hexagonally shaped crystal faces. Al-

Figure 2. Rectangular step-cut green beryl from the Volyn pegmatite, 190.00 ct and 28.55 × 39.02 × 21.71 mm, with a rough unpolished table containing etch pits. Faceting and photo by Konstantyn Zalizko.

Figure 3. Map of the major tectonic units of Ukraine (based on the geological map in Shestopalov et al., 2020, and from Wikimedia Commons) with the Ukrainian Precambrian Shield, part of the East European Platform. Ukraine's two gem beryl occurrences: heliodor in the Volyn pegmatite field in the southwest of the Korosten Pluton and emerald at Kruta Balka, are each indicated with a star.

though dissolution of early precipitated minerals during a later stage is frequently observed in pegmatites (Černý, 2002; London, 2008), these features together with the yellow-green color and their size are diagnostic for Volyn beryl. In large crystals, they are visible without magnification, and in smaller crystals they can be seen with the aid of a loupe or optical microscope.

This study presents an investigation of the morphology of the etch pits on prismatic and basal faces in a number of beryl specimens from Volyn by means of scanning electron microscopy (SEM), which helped to identify the origin of uncut stones, extending the work of Kurumathoor and Franz (2018) on etch pits as a provenance indicator. The nomenclature for etch pits follows from that work: F-type = flat bottom, which originate at point defects; P-type = pointed bottom, which originate at linear defects (i.e., edge and screw dislocations); H-type = hollow, with walls almost perpendicular to a face and bottom that is not visible; and C-type = canoe-shaped.

GEOLOGICAL SETTING

The Volyn pegmatites are genetically and spatially connected with granites of the Korosten plutonic complex in the northwest Ukrainian shield. This pluton crops out over an area of approximately 15,000 km^2 and has intrusion ages of 1800–1760 Ma (figure 3; Shumlyanskyy et al., 2017, 2021). Its country rocks are high-grade migmatic gneisses. In the Khoroshiv region at its western margin, pegmatites are found in a contact zone between granite and gabbroic rocks over a distance of 22 km and a width of 300 to 1500 m (e.g., Lazarenko et al., 1973; Koshil et al., 1991; Ivanovich and Alekseevich, 2007). Miarolitic cavities, produced during the late-stage crystallization by fluids, occur all along the edges of the pluton. The southern and eastern sides have been test-mined for quartz.

The pegmatites belong to the category of shallow pegmatites, fully differentiated, and are irregularly distributed in the granites (Ivanovich and Alekseevich, 2007). According to the nomenclature of Černý and Ercit (2005) and Linnen et al. (2012), they belong to the

miarolitic interior-type of the niobium-, yttrium-, and fluorine-enriched family. They reach a size of several tens of meters; individual pegmatite bodies are typically about 30 m by 40 to 45 m wide (Kalyuzhnyi et al., 1971; Lyckberg, 2005; Ivanovich and Alekseevich, 2007). The pegmatites contain large miarolitic pockets and are referred to in the Ukrainian literature as "chamber pegmatites." They are zoned around an open cavity, which can reach a volume of approximately 40 m^3 and in extreme cases up to 4000 m^3 (Lyckberg et al., 2009).

A cross section of a pegmatite is shown in figure 4. Quartz crystals one or two meters in size, most often as smoky quartz, grew from the hanging wall into the chamber. The floor is covered with quartz that has fallen down, as well as smaller crystals of mica, topaz, beryl, and albite. Chambers in which beryl and topaz occur together as large crystals are the exception in these deposits, because during the multistage crystallization conditions they can replace each other. The footwall of the chambers consists of a strongly leached feldspar-rich horizon up to 36 m deep (Lyckberg et al., 2009) where quartz was dissolved, and further down lies a zone of broken-up pegmatite. New mineral formations in this zone include albite, siderite, topaz, fluorite, beryl (rarely), and phenakite. The zones around the chamber are a quartz core above the chamber, then a more or less concentric feldspar zone, a blocky quartz-feldspar zone with large pegmatitic crystals, and next to the granite a zone with graphic-textured quartz-feldspar intergrowths.

Some of the chambers were destroyed forming a breccia, which consists of broken crystals and rock fragments, cemented by quartz, opal, chalcedony,

Figure 4. Cross section of pegmatite number 487 from the Volyn pegmatite field, showing the different zones. The strongly leached feldspar-rich horizon below the chamber is typical, as is a quartz core above the chamber. The pegmatite measures approximately 12 m × 7.5 m, and the chamber is approximately 5 m × 2 m wide. The vertical scale on the far left represents depth in meters. Modified by D. Lyckberg after © Volyn Quartz Samotsvety Company.

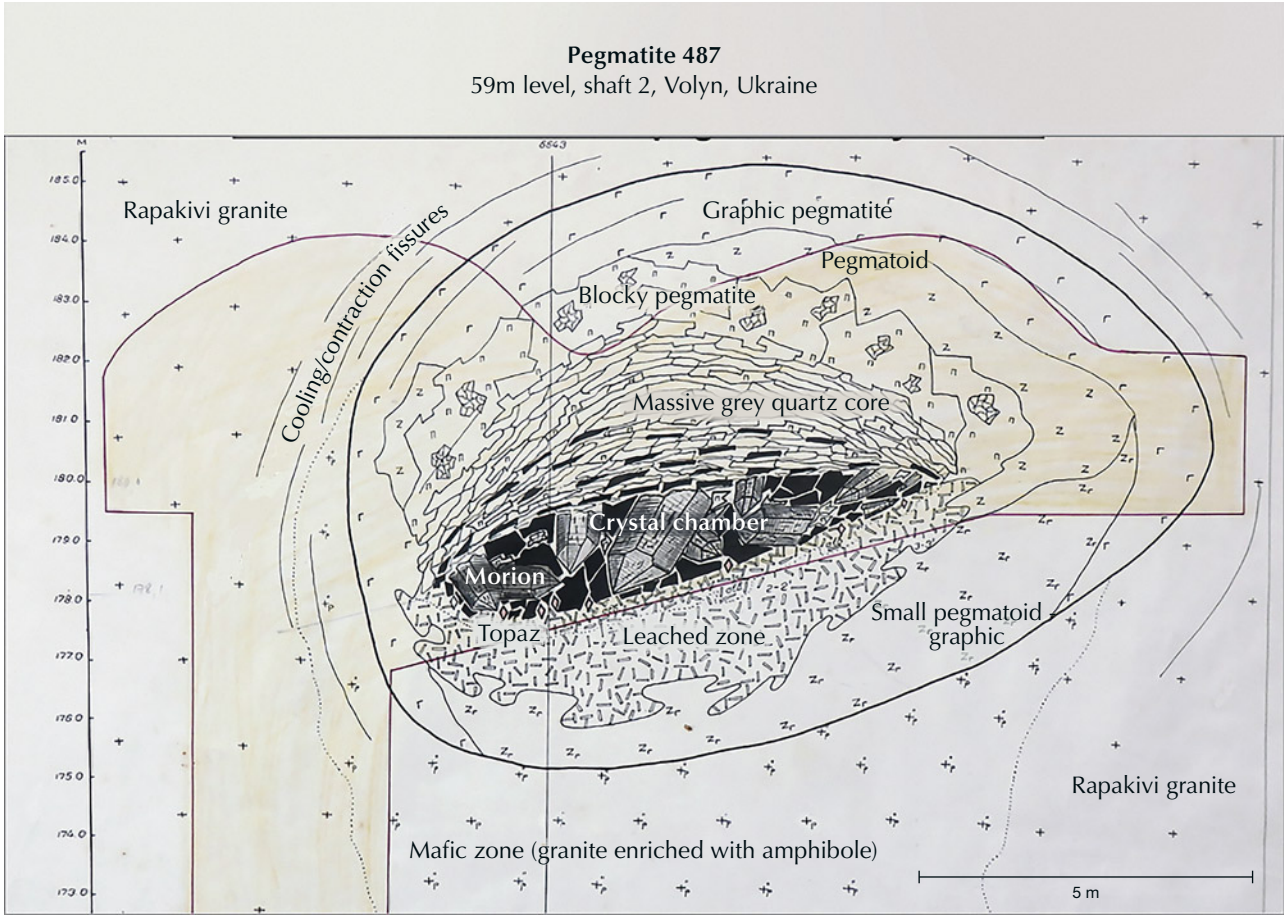

and clay minerals. Pseudomorph replacements of beryl, which now consist of opal, muscovite, bertrandite, buddingtonite, and minor amounts of euclase, albite, potassium feldspar, columbite, pyrite, barite, rare earth element minerals, and organic matter, occur in the breccia (Bartoshinskiy et al., 1969; Franz et al., 2017). The authors recently obtained another sample of a beryl pseudomorph, which contains siderite next to the beryllium minerals bertrandite and euclase, pointing to a variable fluid composition during the latest alteration stages. We also obtained a sample with a pseudomorph of white mica replacing topaz, which again shows the importance of a late alteration stage for the gemstones.

Based on fluid inclusion studies, the pegmatites crystallized at a high fluid pressure, first in a closed system (from 600° to 390°C) and then during cooling in an open system (at 365° ± 15°C) at a depth of 2.0 to 2.5 km (Lukashev, 1976; Kalyuzhnyi et al., 1971; Voznyak, 2007; Voznyak et al., 2012).

Another very special feature of these pegmatites is the occurrence of an organic matter called kerite. It is found within the cavities, attached to feldspar and topaz. It was interpreted as an example of abiogenic (of inorganic origin) formation (Ginzburg et al., 1987; Luk'yanova et al., 1992)—in other words, inorganic synthesis of fibrous carbon hydrates in the cooling stage of the pegmatites. They were later reinterpreted as fossil cyanobacteria (Gorlenko et al., 2000; Zhmur, 2003) from a geyser-type deposit. Recent investigations (Franz et al., 2022, 2023) have also identified a number of different fossils, some of them fungi-like. Filamentous fossils and remnants of former biofilms were also identified in etch pits of beryl.

PREVIOUS WORK ON VOLYN BERYL

Beryl is an accessory mineral found in 2% of the approximately 1500 pegmatite bodies at Volyn. It is present in small amounts in cavity areas, found in clay primarily in the lower sections of the pocket where they once grew on albite (Lyckberg et al., 2009), but their initial location is mostly lost. Beryl crystals are usually sitting in a clay-mica-quartz rock matrix or in a soft clay mass of dominantly kaolinite, as variably oriented individual crystals. Anhedral crystals, measuring no more than 0.5 cm in cross section, also occur in the leached zone under the chamber, where beryl fills cracks and leaching voids in albite.

The Vickers hardness of the Volyn beryl as measured on prismatic faces ranges from 1380 to 1395 kg/mm^2 (Lazarenko et al., 1973), corresponding to 7–8 on the Mohs scale. Volyn beryl is characterized by a relatively low density of 2.65 to 2.75 g/cm^3 (Gurskyi et al., 2006) and low refractive indices of n_o = 1.568–1.570 and n_ε = 1.566–1.567 (Lazarenko et al., 1973).

TABLE 1. Morphological characteristics of Volyn beryl (Lazarenko et al., 1973).

Morphological types	Type 1	Type 2	Type 3	Type 4	Type 5
Color	Brownish green	Light yellow, yellowish green	Greenish yellow, yellowish green	Light green to light blue	Brownish green to yellow
Shape	Prismatic	Long-prismatic, columnar	Needle-shaped, prismatic	Prismatic	Irregular
Other faces, etch pits	Rarely developed {0001} and {11$\bar{2}$1} faces	Deep etch pits; only remants of edges	Curved {11$\bar{2}$1}	Microporous dissolution	Only relics of original faces
External features (rough crystals)	All types: Rectangular and nearly square etch pits on {10$\bar{1}$0} prismatic faces, hexagonal etch pits on {0001} basal planes, and triangular hillocks between prismatic faces and on transition from prismatic faces to pyramidal faces				

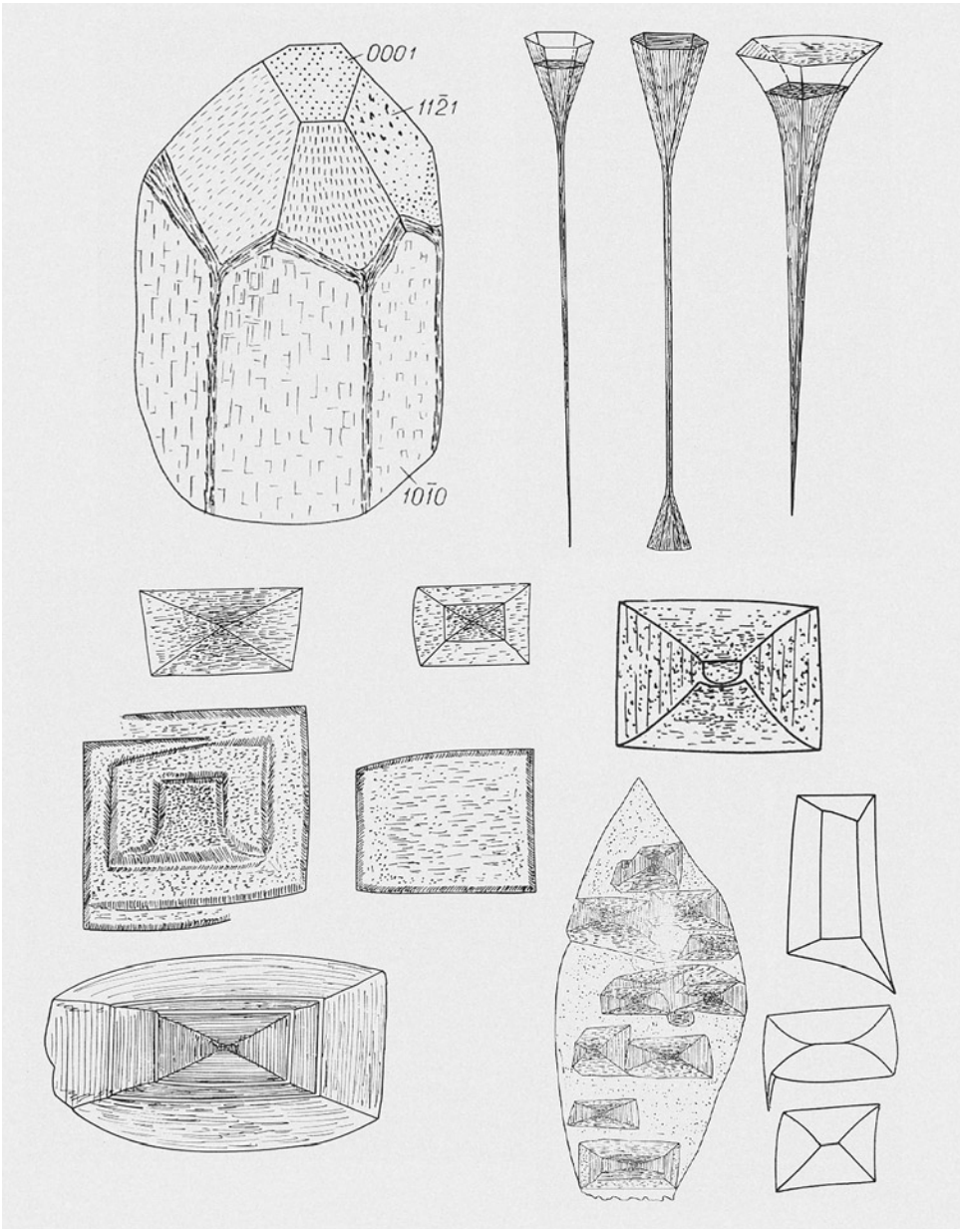

Figure 5. Crystal drawings, reproduced from Bartoshinskiy et al. (1969), showing the typical crystal habit with Miller indices of the common faces (top left), spectacular long funnel-shaped etch pits (ending in thin tubes) on the pinacoidal face (top right) and the typical P-type and F-type etch pits on the first-order prismatic face. The outline can be symmetrical or asymmetrical, and F-types can overlap each other. No scale was given in the original publication.

Only a few chemical analyses of Volyn beryl are available in the literature (Lazarenko et al., 1973; Khomenko et al., 2007; Voznyak et al., 2012). The low contents of sodium (≤0.10 wt.%), lithium (≤0.02 wt.%), cesium (≤0.24 wt.%), iron(II) (≤0.29 wt.%), and magnesium (≤0.03 wt.%), as well as the relatively high Fe^{3+}/Fe^{2+} ratios (on average near 7:1), are characteristic for Volyn beryl. Titanium, manganese, chromium, vanadium, potassium, calcium, gallium, niobium, molybdenum, and barium were reported as minor elements, mostly below or near 0.01 wt.%.

Lazarenko et al. (1973) described different stages of the dissolution of beryl, which produced five morphological types of columnar-prismatic, occasionally spicular beryl crystals (table 1), with characteristically sculptured crystal faces as well as systems of dissolution cones (so-called etch channels). Basal faces are rare. Bartoshinskiy et al. (1969) showed rectangular F- and P-type etch pits with a partly curved outline on the first-order prismatic face and spectacular long, tubular etch pits on the pinacoidal face (figure 5).

The nature of the typical color for Volyn heliodor was studied by Khomenko et al. (2007, 2010) using optical spectroscopy. Variations in the color of Volyn beryl are due to the intensity of the absorption seen in the slope from 28000 to 22000 cm^{-1} of the strong

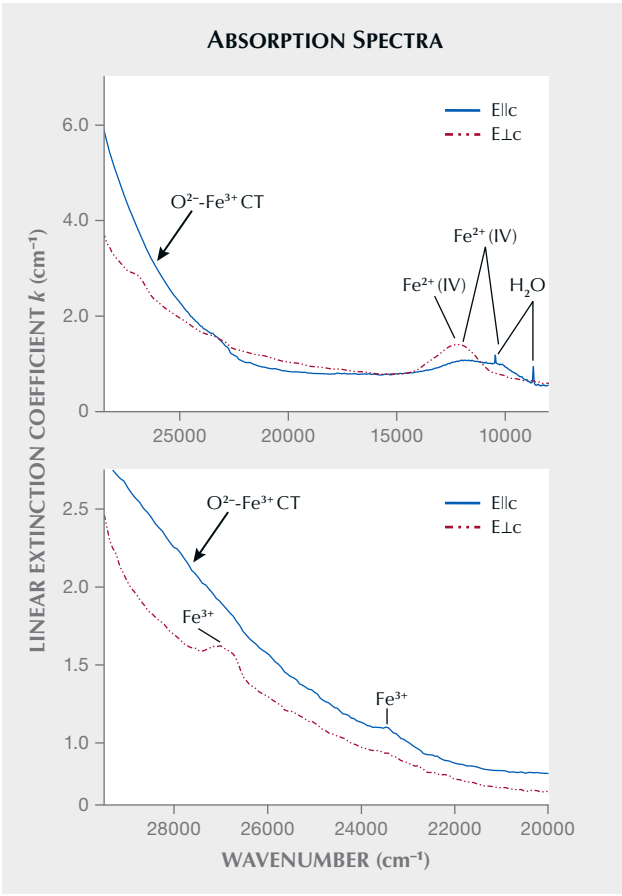

Figure 6. A: Representative polarized optical absorption spectra of a weakly colored yellow-green beryl from Volyn. Linear extinction coefficient k *(cm^{-1}) is the absorption coefficient of a sample 1 cm thick. Arrows point to a strong long-wave tail of the O^{2-}-Fe^{3+} charge transfer (CT) in the UV region and the weak Fe^{2+} and H_2O bands in the NIR region. B: Absorption along the long-wavelength slope of a strong O^{2-}-Fe^{3+} charge transfer band that causes yellow color in the polarized spectra of heliodor. Spin-forbidden absorption bands of Fe^{3+} ions are labeled with arrows; modified from Khomenko et al. (2007, 2010).*

UV absorption, caused by the O^{2-}-Fe^{3+} charge transfer in structural or interstitial positions near the cationic vacancies (figure 6). This slope covers the blue absorption at approximately 450–470 nm (22222–21276 cm^{-1}). Fe^{2+} ions do not affect the color of Volyn heliodors, confirming results of previous spectroscopic investigations by Wood and Nassau (1968), Schmetzer et al. (1975), and Platonov et al. (1984, 2016).

Volyn beryl's color varies from saturated brownish green to light yellow-green (figures 1 and 2). Most of the gem-quality crystals can be regarded as typical heliodor with a yellowish shade of variable intensity (rare greenish blue crystals are displayed in the Museum of Precious and Decorative Stones; Vasylyshyn et al., 2001). Although some reproductions of crystals from Volyn show an intense green color resembling that of emerald, this is purely a matter of color reproduction: Typical emerald color is not reported from Volyn crystals, in line with the absence of chromium and vanadium. Ukraine's only emerald occurrence is Kruta Balka (Franz et al., 2020), and the attribution of emerald to Volyn in Grundmann and Giuliani (2002) is probably erroneous. Morganite has not been reported from Ukraine, either.

MATERIALS AND METHODS

For SEM investigation of the etch pits, nine light yellowish green beryl crystals were selected from the collection of the Institute of Geochemistry, Mineralogy and Ore Formation of the National Academy of Sciences of Ukraine (IGMOF NASU) in Kyiv, along with three nearly colorless prismatic crystals (collected by author GF from the mine tailings in 2008) with a partly developed pinacoidal face.

SEM and energy-dispersive X-ray spectroscopy (EDS) were performed using a JEOL JSM-6700F field emission scanning electron microscope equipped with a JED-2300 EDS spectrometer at IGMOF NASU. The spectra were collected with an accelerating voltage of 15 kV and a beam current of 0.65 nA. Operating conditions for each analysis were identical. The samples were cleaned in an ultrasonic bath and then sputtered with a platinum layer of 15 nm thickness. The three nearly colorless crystals were carbon coated and investigated at the Central Facility for Electron Microscopy (ZELMI), Technical University Berlin, using a Hitachi SU8030 cold field emission SEM equipped with an EDAX Octane-A Plus 30 mm^2 silicon drift detector for qualitative EDS analysis. Some images were obtained in combination with a backscattered electron (BSE) and SE detector.

Standard gemological properties were investigated on another 16 rough beryl crystals (mineralogical collection of IGMOF NASU) and 20 faceted beryls (private collection of O. Vyshnevskyi) from the Volyn pegmatite field. For refractive index and birefringence measurements, we used an Eickhorst GemLED refractometer. Sartorius CP 224 S analytical lab balances equipped with a hydrostatic attachment were used for specific gravity (YDK01MS Density Determination Kit), using distilled water as fluid. The color of the samples was graded using a GIA GemSet in strong, diffuse daylight.

TABLE 2. Gemological characteristics of Volyn beryl.

Color	Very light to medium yellowish green	Very light to strongly yellowish green	Very light to medium green-yellow
Refractive index	n_ω = 1.569–1.570 n_ε = 1.562–1.564	n_ω = 1.568–1.571 n_ε = 1.562–1.566	n_ω = 1.568–1.571 n_ε = 1.562–1.566
Birefringence	0.006–0.008	0.005–0.006	0.005–0.006
Specific gravity			
Rough crystals (16)		2.62–2.70	
Faceted stones (20)		2.66–2.70	
Internal features	Crystals, liquid (fluid) inclusions, fingerprints, etch tubes, fractures		

RESULTS

Gemological Characteristics. The standard gemological properties of the 16 rough and 20 faceted samples are summarized in table 2. All were transparent to translucent, and none showed fluorescence under short- and long-wave UV light. Their refractive indices of 1.568–1.571 (n_ω) and 1.562–1.566 (n_ε) and birefringence values of 0.005–0.008 were typical for natural beryl. Samples with stronger yellowish hue showed slightly lower birefringence. Eye-clean rough crystals, as well as all faceted stones, had a specific gravity in the range of 2.66–2.70. Translucent rough beryl had a lower specific gravity range of 2.62–2.65, which may be due to numerous fluid inclusions. Solid inclusions with a size of tens to hundreds of micrometers, brought to the surface in polished sections, were identified by EDS analysis as albite, microcline, muscovite, columbite, iron sulfide, titanium oxide, and iron oxide/hydroxide (possibly goethite).

Morphology of Etch Pits. In general, the "negative faces" of an etch pit follow the symmetry pattern of the crystal. The nomenclature for the description is outlined in figure 7. Faces of the etch pits can be

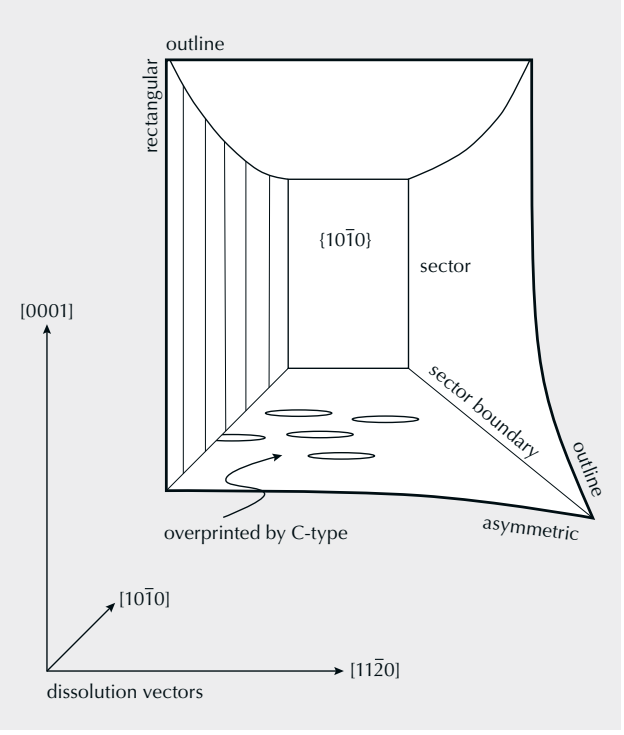

Figure 7. Nomenclature for the description of etch pits, shown for F-type (flat bottom, originating from point defects) on the first-order prism. P-type etch pits show the same features, except that the bottom is pointed. The outline of the etch pit indicates the relative dissolution vectors in the directions parallel and perpendicular to the c*-axis. If the vectors do not change with increasing depth, sectors with straight boundaries are formed. If the dissolution vectors change relative to each other, sector boundaries become curved toward an hourglass shape. Stepped sectors indicate discontinuities in the dissolution velocity. An asymmetric outline indicates heterogeneous dissolution within a growing etch pit. Etch pits of one kind or one generation can be overprinted by another type.*

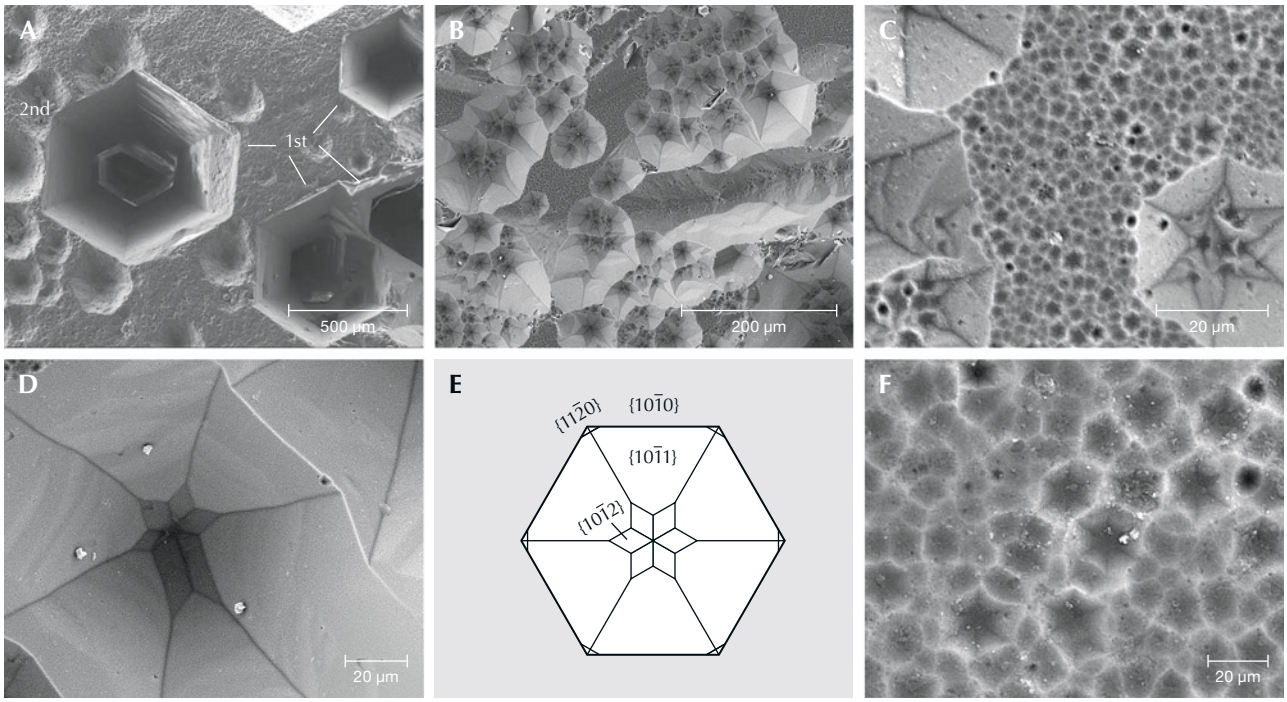

Figure 8. SEM images of Volyn beryl crystals with etch pits on {0001}. A: Deep first-order P-type etch pits (transitional to H-type) with no steps, straight, regular in outline, and up to 500 µm in diameter together with irregular second-order P-type etch pits approximately 50 µm in diameter. B: Second-order P-type etch pits overlapping each other. C: Second- and third-order P-type etch pits. D: Star-like bottom in a second-order P-type etch pit, produced by dissolution following first the {10$\bar{1}$0} first-order prismatic face, then in the deep part the {11$\bar{2}$0} second-order prismatic face. E: Diagram of a P-type etch pit; the negative crystal produced by dissolution shows the {10$\bar{1}$0} first-order prismatic face with the {10$\bar{1}$1} in the upper part and at the bottom the {10$\bar{1}$2} first-order hexagonal dipyramidal faces. This indicates a change in the relative dissolution velocity with increasing depth. F: Third-order P-type etch pits, with about 1 to 3 µm diameter.

even or stepped; outlines of an etch pit on the crystal face can be straight or curved, symmetrical or asymmetrical.

Rectangular etch pits on first-order prismatic faces {10$\bar{1}$0} and hexagonal etch pits on the basal planes {0001} were formed by dissolution. Pyramidal faces are rarely developed on the investigated crystals. Etch pits on {0001} are P-type; however, some with very steep faces are transitional to H-type (figure 8). We observe three orders of magnitude: First-order etch pits are up to 500 µm in diameter and have a mostly straight hexagonal outline (figure 8A). Second-order etch pits are on the order of 50 µm wide, with a less regular outline, partly overlapping each other (figure 8, B and C). Many of these show at their bottom a star-like pattern (figure 8D), produced by a change from dissolution parallel to the first-order prismatic face {10$\bar{1}$0} to dissolution parallel to the second-order prismatic face {11$\bar{2}$1} (figure 8E). The negative crystal produced by dissolution shows the {10$\bar{1}$0} first-order prismatic face with the {10$\bar{1}$2} and {10$\bar{1}$1} first-order hexagonal dipyramidal faces. Third-order etch pits are 1 to 3 µm wide, irregular in outline and very abundant, covering all of {0001} (figure 8, C and F).

Figure 9 shows etch pits on the first-order prism {10$\bar{1}$0} of the beryl crystals. These etch pits are rectangular, with their long side parallel to the *c*-axis (figure 9A), perpendicular (figure 9B), or nearly square (figure 9C). Similar to {0001}, F-type etch pits were observed in three orders of magnitude; however, P-types are much rarer and only observed in first-order, whereas F-types dominate and there is a more or less continuous spectrum for second- and third-order types. In addition, there are small C-type etch pits, which can be oriented perpendicular to the *c*-axis (figure 9, D and E) or parallel to the *c*-axis (figure 9, F and G). First-order P-types with stepped sides can be strongly elongated parallel to the *c*-axis (figure 9, D and E). F-type etch pits show a smooth curvature of the edges (figure 9G), which was also observed in P-types (figure 9B).

Edges between two first-order prisms are characterized by the presence of triangular hillocks, formed by dissolution of the prismatic faces (figure 1B and figure 10). Pyramidal faces were only observed in one

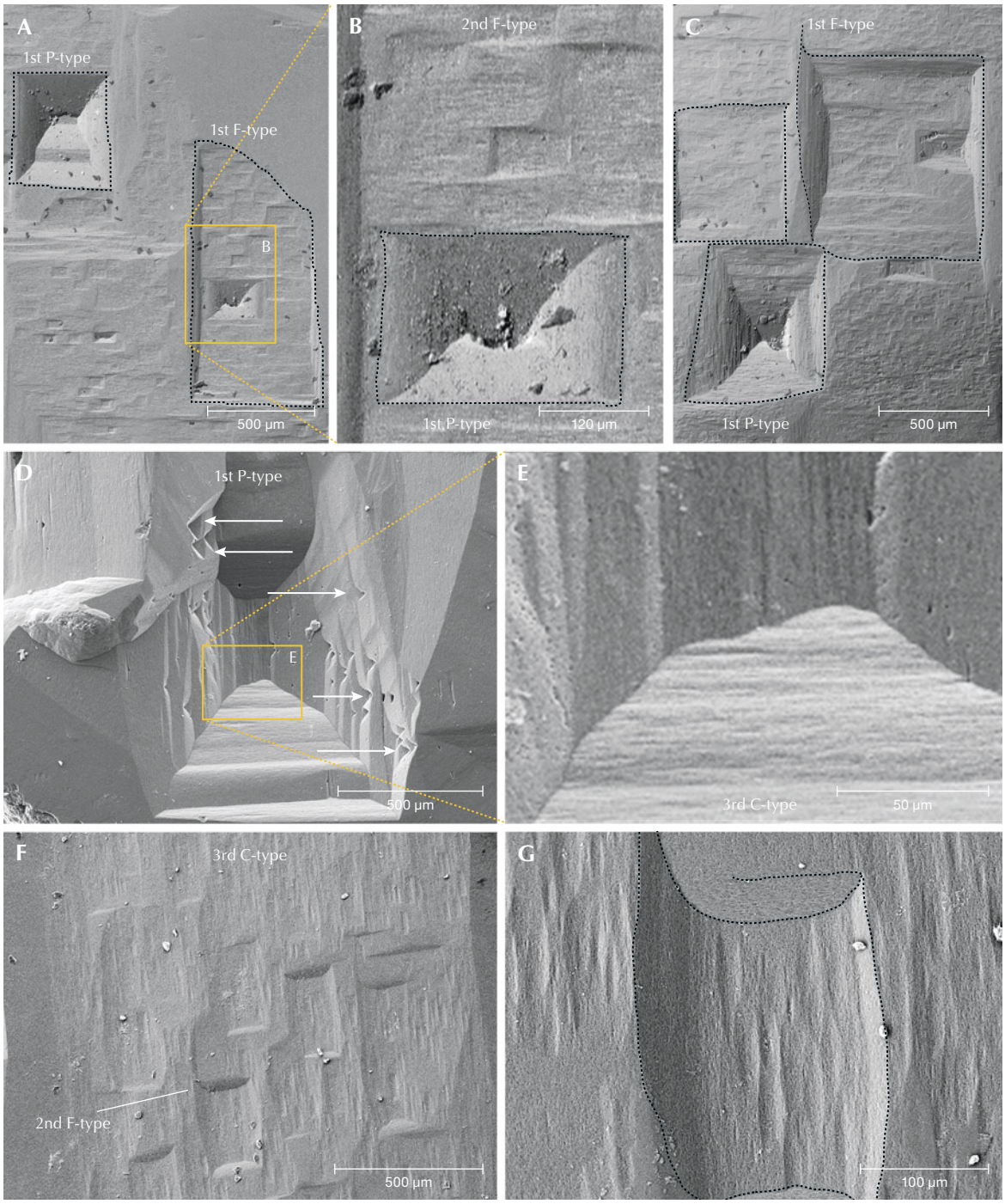

Figure 9. SEM images of Volyn beryl crystals with etch pits on first-order prismatic faces {10$\bar{1}$0}, with the orientation of the c*-axis nearly vertical. Some etch pits are outlined (black dotted lines). A: Rectangular first-order P-type etch pit and asymmetric first-order (1st) F-type etch pit (approximately 500 µm × 1000 µm) with long edge parallel to the* c*-axis. Note the second-order (2nd) approximately 50 µm × 100 µm wide F-type etch pits within first-order F-type etch pit. B: Rectangular symmetric first-order P-type etch pit with smoothly curved, hourglass-shaped sector boundaries. C: Two large first-order F-type etch pits, and an asymmetrical first-order P-type etch pit, overprinted by very flat second- to third-order F-type etch pits. D: Stepped first-order P-type etch pit with bottom elongated into a line. Note the small triangular etch pits in the left and right sector walls (arrows). E: Lower sector wall with third-order C-type etch pit, oriented perpendicular to the* c*-axis. F: Second-order F-type etch pits with large, asymmetric third-order C-type etch pits oriented parallel to the* c*-axis (magnified in G).*

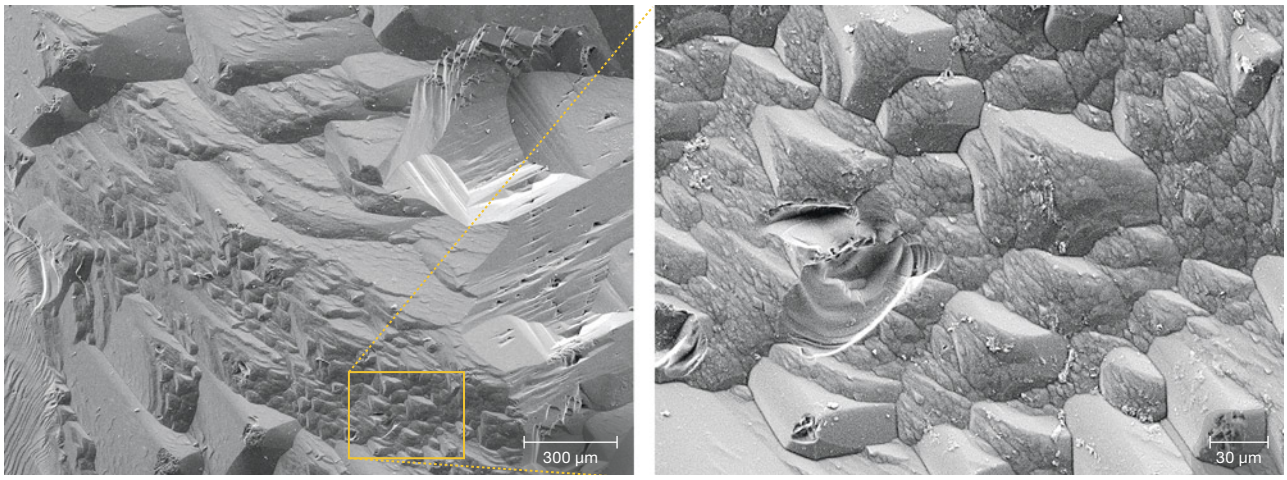

Figure 10. SEM image (left) of the edge between two prism faces, forming triangular hillocks, magnified on the right.

crystal and contained triangular steps (figure 11). On the steps, small third-order F-type etch pits developed.

Analysis of the crystals' surfaces yielded more information about the dissolution process and the components in the dissolving fluid. The faces show a porosity, both outside and inside the etch pits (figure 12) and also within the small C-type etch pits. Individual pores show no crystallographic outline and are on the order of several hundred nanometers, mostly elongated parallel to the *c*-axis. Very small grains of a titanium dioxide polymorph and gold (with minor contents of silver, copper, and iron as determined by EDS) were observed (figure 12D), as well as particles consisting of a mixture of chloride and sulfate crystals and a particle with light rare earth elements and phosphorous.

DISCUSSION

On a crystal face, the distinction between growth features and dissolution features is based mainly on the observation that growth features, such as growth hillocks, are positive (on the basal plane with a hexagonal shape), rising up on top of each other in stepwise fashion (Sahama, 1966), whereas pits that extend down into the crystal are negative and indicate dissolution. Flamini et al. (1983) showed SEM images of growth features on red (manganese-bearing) beryl from Utah. The features described above on the pinacoid and the prism of Volyn beryl are all interpreted as dissolution features. Phenomena observed at crystal edges and the transition from the prism to the pinacoid are less clear, and we propose that for a provenance study

Figure 11. Left: SEM image of dissolution features on the transition from prismatic face (lower part, with rectangular F-type etch pits) to pyramidal face (upper right), with the formation of triangular hillocks. Right: Small etch pits (indicated by arrows) formed parallel to the larger F-type etch pits on the prismatic face.

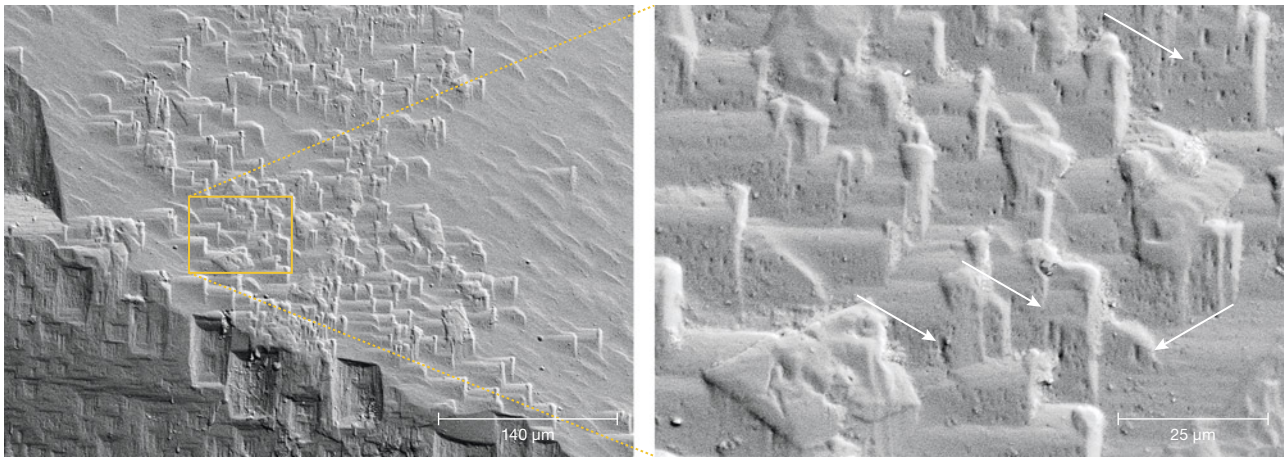

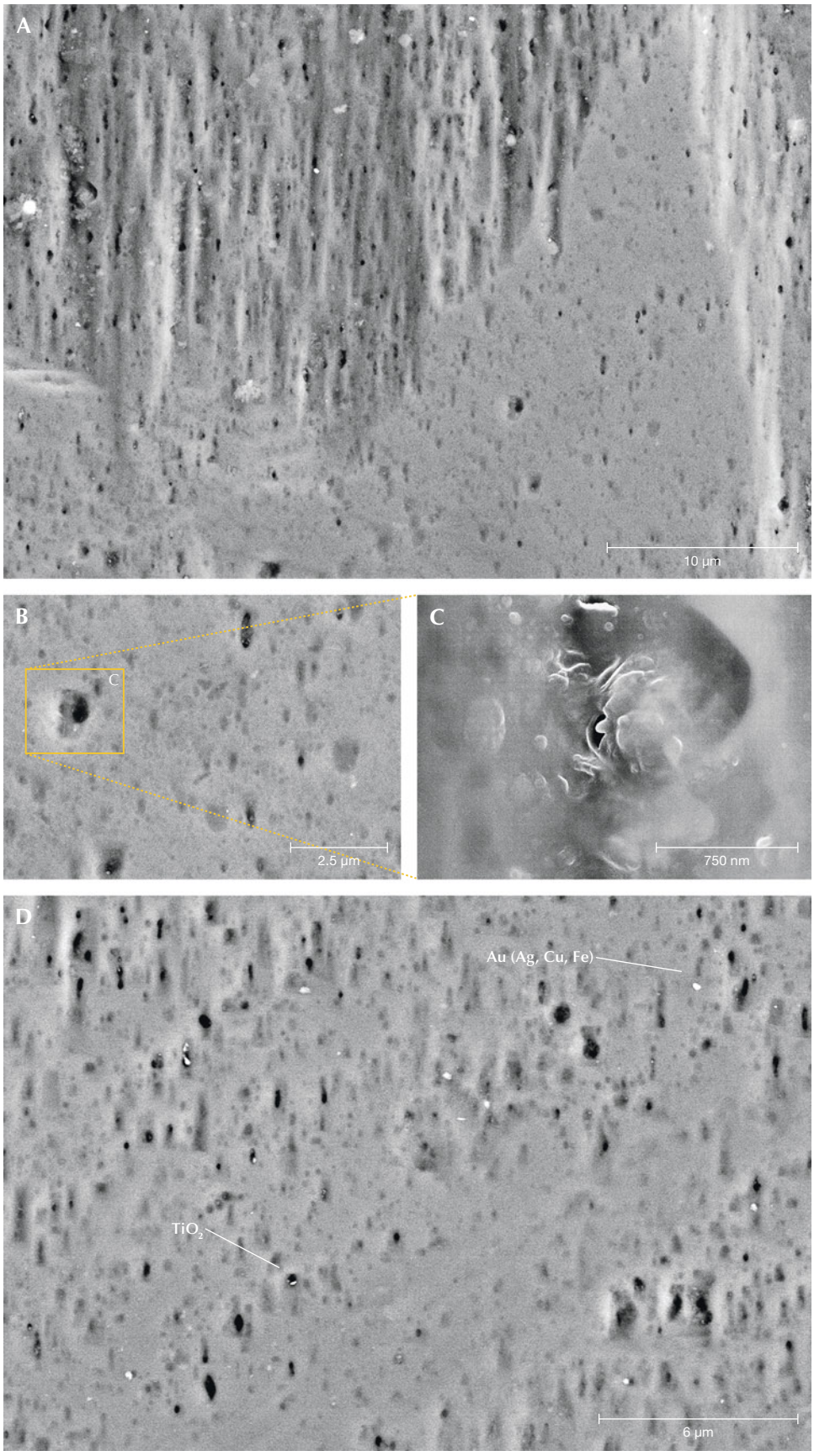

Figure 12. Combined SEM-BSE images of enlarged areas of a prism face, showing small-scale porosity. A: The edge of an etch pit with elongated C-type etch pits. The smooth surface is a prism face near the etch pit. B and C: Enlarged part of the prism face, showing anhedral pores measuring several hundred nanometers. D: A surface with very small grains of gold with silver, copper, and iron impurities, as well as titanium dioxide (chemical composition determined by EDS).

only the pinacoid and the first-order prism should be used.

Dissolution of a mineral can be considered as "negative growth." As growth is generally described by growth laws (e.g., Philpotts and Ague, 2022), similarly we can describe dissolution by "negative growth laws." On a crystal face, dissolution is first dominated by the number of defects (i.e., dislocation-controlled). Removal of atoms is energetically favored at defects compared to an ideal surface. At point defects, the defect disappears and removal of atoms produces steps on the crystal's face in two directions. On a linear defect, the defect extends in the third dimension into the crystal and removal of atoms continues in three dimensions. Once a deep etch pit has formed, dissolution can be rate-determined by diffusion of the components in solution out of the etch pit, and it is then diffusion-controlled. This is what is seen on the pinacoidal face. There are a few first-order etch pits, due to a small number of large screw dislocation bundles, which were formed parallel to the *c*-axis during growth of the crystal. They can probably extend deep into the crystal as etch channels (Bartoshinskiy et al., 1969).

We interpret the second-order etch pits as due to smaller screw dislocations, which are more frequent (figure 8A) and formed a negative first-order prism. When these etch pits became deep, the dislocation-controlled dissolution was followed by a diffusion-controlled dissolution, and the negative crystal ends with the $\{10\bar{1}2\}$ and $\{10\bar{1}1\}$ first-order hexagonal dipyramidal faces. Relative dissolution velocity is—as estimated from the shape and depth of the etch pits—in the sequence of the directions [0001] > $[11\bar{2}0]$ > $[10\bar{1}0]$. The deep channels (figure 5) shown by Bartoshinskiy et al. (1969) demonstrate that [0001] is a preferred direction for dissolution. Very deep P-type etch pits are also shown in figure 8A, where the bottom is no longer visible. In the diagram in figure 8E, the negative crystal produced by dissolution is shown in the upper part the outline of the $\{10\bar{1}0\}$ first-order prismatic face with the $\{10\bar{1}1\}$ hexagonal dipyramidal faces. This indicates faster dissolution in $[11\bar{2}0]$ compared to $[10\bar{1}0]$, leaving traces of the first-order prismatic faces. At the bottom (i.e., with increasing depth), a change is seen from the $\{10\bar{1}1\}$ first-order hexagonal dipyramidal faces to the $\{10\bar{1}2\}$ hexagonal dipyramidal faces (figure 8, C and D). This indicates a change in the relative dissolution velocity with increasing depth. Therefore, at the end of the etch pit, the sequence of relative velocities is [0001] > $[10\bar{1}0]$ > $[11\bar{2}0]$, which also implies that dissolution in $[11\bar{2}0]$ is not very different from that in $[10\bar{1}0]$.

Third-order etch pits are very abundant, covering the basal plane completely and also occurring within second-order etch pits (figure 8, C and F). Such a high number of growth dislocations seems unlikely, and we propose that dissolution on these faces is controlled by the crystal structure of beryl with its pronounced channels parallel to the *c*-axis. Demianets et al. (2006) determined by atomic force microscopy that experimentally produced hydrothermal beryl shows growth hills on the pinacoidal face, with a separation distance of approximately 0.2 µm. The cavities around such growth hills might be correlated with the sites where dissolution is effective in the absence of dislocations, producing the third-order etch pits (figure 8F). The centers of the Si_6O_{18} rings within the beryl structure aligned with the basal planes are sites of preferential removal of atoms, supported by the fact that first-order etch pits are very deep and can extend into the long, funnel-shaped tubes (figure 5; Bartoshinskiy et al., 1969; Lazarenko et al., 1973) perpendicular to the Si_6O_{18} rings. This is also in line with the sodium-poor composition of Volyn beryl. Sodium would be situated within the channels, generally bound to a tetrahedral site with a stronger bond than water and could thus prevent strong dissolution in [0001].

On the first-order prismatic faces, P-type etch pits are rare and most are large, first-order P-types (figure 9), indicating relatively few screw dislocations perpendicular to the *c*-axis. Prismatic faces are dominated by F-type etch pits, associated with point defects (substituting atoms, vacancies, and interstitial atoms). These etch pits are very abundant, often covering the whole face and overlapping each other (figure 1). They range in size from a centimeter down to several micrometers (figure 9), and though we classified them as first- and second-order etch pits, there is more or less a continuum in size. The outline is rectangular, elongated perpendicular or parallel to the *c*-axis, or nearly square, indicating essentially equal dissolution velocities in both directions. The sector boundaries are mostly straight, with equal dissolution velocities in both directions, but some show curved boundaries, indicating continuously changing dissolution velocities, also observed in P-type etch pits (figure 9B). First-order etch pits can also be asymmetrical.

Our investigations also yielded some information about the fluid phase, which caused the dissolution. This fluid must have been able to transport elements

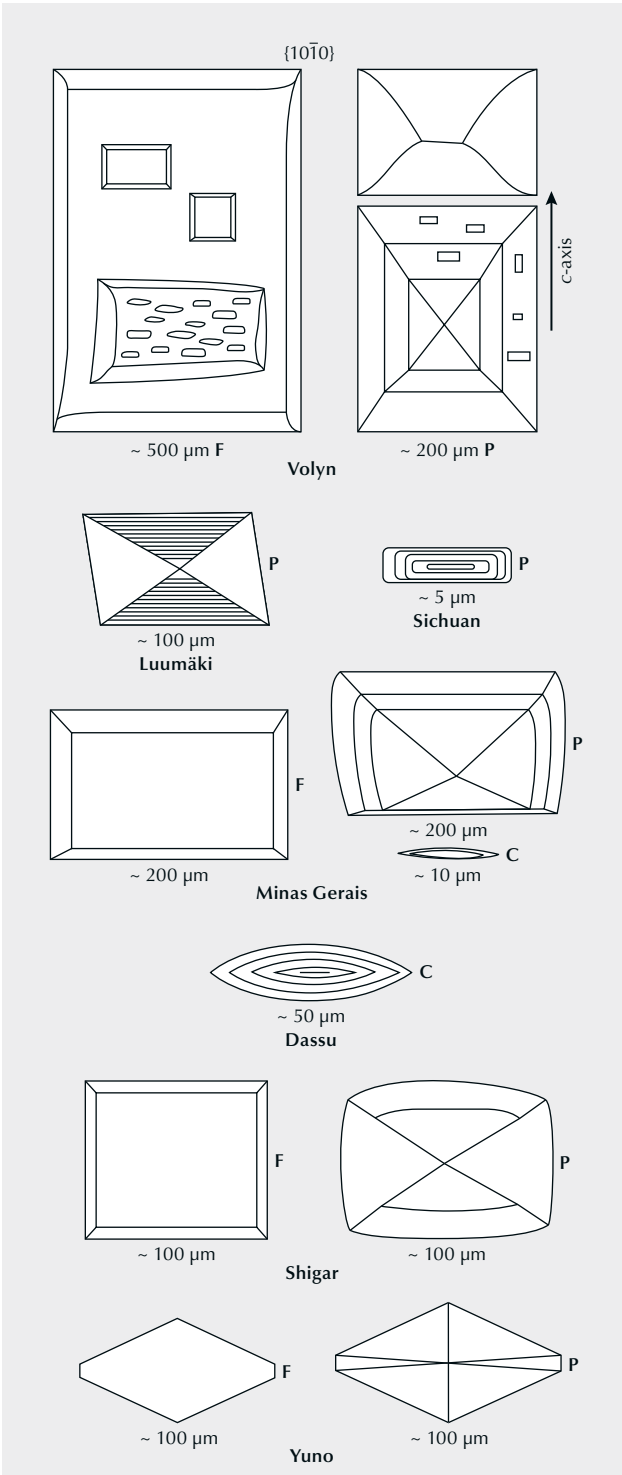

Figure 13. Diagrams of etch pits on {10$\bar{1}$0} of heliodor from Volyn compared to heliodor from Luumäki (Finland) and aquamarine from Sichuan (China), Minas Gerais (Brazil), Dassu, Shigar, and Yuno (Himalayas), from Kurumathoor and Franz (2018). F- and P-type etch pits are larger on crystals from Volyn and overlap each other, but note that they can also be asymmetrical. Within F-type etch pits, C-type etch pits oriented perpendicular to the c-axis are larger and more irregular in outline than on crystals from Minas Gerais. In P-type etch pits on crystals from Luumäki, abundant steps were identified, whereas the steps in crystals from Volyn are less frequent or missing, and sector boundaries can be curved.

such as titanium, rare earth elements, and even gold (figure 12D). Furthermore, we know from the locality that in these niobium-, yttrium-, and fluorine-rich pegmatites, fluorine is a major component, as shown by the abundance of topaz as a typical gemstone, by fluorite as an accessory mineral, and by the occurrence of fluorine-rich muscovite (Franz et al., 2017). Beryl and topaz can be related to each other by the chemical equilibrium

$$Be_3Al_2Si_6O_{18} + 28\ HF \rightleftharpoons Al_2F_2SiO_4 + 3\ BeF_2^{fluid} + 5\ SiF_4^{fluid}\ 14\ H_2O$$

where beryllium fluoride and silicon fluoride are fluid species. This chemical equilibrium might explain why either beryl or topaz crystallized in the chambers, but rarely both, and it also hints toward a fluorine-rich fluid phase for the late-stage dissolution of the beryl. Lyckberg et al. (2009) noted that when topaz and beryl occur together, one grows at the expense of the other, which supports the interpretation inferred from the chemical equilibrium above.

The large gem-quality crystals with their dissolution phenomena on the surfaces show that possible products of newly formed minerals during incongruent dissolution have been transported away. In other words, we are dealing with an open system. Possible remnants of beryl dissolution as clay-like material are observed in some etch pits, but it is not yet clear whether this material is a product of the dissolution of the beryl or contamination from a late-stage hydrothermal process of other minerals such as feldspar.

The shape and size of the etch pits on Volyn beryl are different from those of other pegmatitic beryls (figure 13; Kurumathoor and Franz, 2018) and may well help to identify uncut crystals. A characteristic feature in particular is that F-type etch pits are much larger (figures 8 and 9) compared to beryl from most other localities. They frequently overlap each other (figures 1, 8, and 9), which is rarely observed in beryl from other localities. The different dissolution stages of the Volyn beryl with varying acidity-alkalinity described in the literature (Barthoshinskiy et al., 1969;

Lazarenko et al., 1973) might be correlated with our observation of first-, second-, and third-order etch pits. The degree of etching is quite variable on different crystals, and it even varies from pegmatite to pegmatite (Lyckberg et al., 2009).

The crystal from Minas Gerais in figure 13 shows similarly large F- and P-type etch pits and also small third-order C-type etch pits within F-type etch pits. At Volyn, however, the C-type etch pits are much larger, more abundant, and less regular in outline (figure 13A). C- and P-type etch pits measuring from 5 up to 50 µm, as observed in crystals from Dassu (Himalayas) and China, were not found in Volyn beryl, nor was the orthorhombic outline of F- and P-type etch pits in crystals from Yuno (Himalayas). Aquamarine from Shigar (Himalayas) shows P-type etch pits with a curved outline, which is not observed in the Volyn crystals, but its flat F-type etch pits are similar. Although the geological background of Volyn beryl is most similar to that from Luumäki, Finland (Lahti and Kinnunen, 1993; Lyckberg, 2004), with a similar heliodor color and a similar relation to a Precambrian anorthosite pluton, the etch pits on the prism faces are quite different (figure 13). On the crystals from Luumäki, only P-type etch pits were observed in Kurumathoor and Franz (2018), with an oblique outline and frequent steps. It must be noted, however, that for Kurumathoor and Franz (2018) only a small fragment from one crystal was available, which might not be representative for the occurrence. Furthermore, it must be kept in mind that up to now only a few crystals from the different localities could be investigated using SEM. Future research should be concentrated on more crystals from the same localities and on other beryl varieties with different composition (e.g., rich in sodium-magnesium, lithium-cesium, or manganese) that are also from non-pegmatitic environments.

CONCLUSIONS

Beryl crystals from Volyn are associated with the Korosten pluton in the Precambrian Ukrainian Shield. These crystals are of gem quality, exceptional in size, and have excellent color—both the yellow heliodor and the green beryl. They are found in chambers of pegmatites that formed in the cooling and crystallization stages of the pegmatite melt. A special feature of these beryl crystals is the appearance of dissolution features known as etch pits. On the prismatic face, these etch pits are very pronounced and often cover the whole crystal. On the basal face, they form six-sided channels, ending with pyramidal faces or penetrating deep into the crystal. The shape and size of the etch pits are characteristic for the Volyn occurrence and easily distinguish them from beryl crystals from other localities.

ABOUT THE AUTHORS

Dr. Gerhard Franz is a retired professor of mineralogy and petrology at the Institute for Applied Geosciences, Technical University Berlin. Dr. Oleksii Vyshnevskyi and Dr. Volodymyr Khomenko are senior researchers at the Institute of Geochemistry, Mineralogy and Ore Formation of the National Academy of Sciences of Ukraine. Dr. Peter Lyckberg is a researcher and scientific collaborator with the National Museum of Natural History in Luxembourg. Ulrich Gernert is a physics engineer at the Central Facility for Electron Microscopy (ZELMI), Technical University Berlin.

ACKNOWLEDGMENTS

The Alexander von Humboldt Foundation financially supported author V. Khomenko's stay in Berlin in 2022–2023. The Museum for Precious and Decorative Stones in Khoroshiv is thanked for the permission to use the photograph of a beryl crystal in figure 1. We also thank the peer reviewers and editors for handling the manuscript, as well V. Chournousenko for stimulating discussions and for sharing his knowledge about the Volyn pegmatite field.

REFERENCES

Bartoshinskiy Z.V., Matkovskiy O.I., Srebrodolskiy B.I. (1969) Accessory beryl from chamber pegmatites of Ukraine. *Mineralogical Sbornik*, Vol. 23, No. 4, pp. 382–397 [in Russian].

Černý P. (2002) Mineralogy of beryllium in granitic pegmatites. *Reviews in Mineralogy and Geochemistry*, Vol. 50, No. 1, pp. 405–444, http://dx.doi.org/10.2138/rmg.2002.50.10

Černý P., Ercit T.S. (2005) The classification of granitic pegmatites revisited. *Canadian Mineralogist*, Vol. 43, No. 6, pp. 2005–2026, http://dx.doi.org/10.2113/gscanmin.43.6.2005

Demianets L.N., Ivanov-Shitz A.K., Gainutdinov R.V. (2006) Hydrothermal growth of beryl single crystals and morphology of their singular faces. *Inorganic Materials*, Vol. 42, No. 9, pp. 989–995, http://dx.doi.org/10.1134/S0020168506090111

Flamini A., Gastaldi L., Grubessi O., Viticoli S. (1983) Sulle caratteristiche particolari del berillo rosso dell'Utah. *La Gemmologia*, Vol. 9, No. 1/2, pp. 12–20 [in Italian].

Franz G., Khomenko V., Vishnyevskyy A., Wirth R., Struck U., Nissen J., Gernert U., Rocholl A. (2017) Biologically mediated crystallization of buddingtonite in the Paleoproterozoic: Organic-igneous interactions from the Volyn pegmatite, Ukraine. *American Mineralogist*, Vol. 102, No. 10, pp. 2119–2135, http://dx.doi.org/10.2138/am-2017-6055

Franz G., Vyshnevskyi O., Taran M., Khomenko V., Wiedenbeck M., Schiperski F., Nissen J. (2020) A new emerald occurrence from Kruta Balka, Western Peri-Azovian region, Ukraine: Implications for understanding the crystal chemistry of emerald. *American Mineralogist*, Vol. 105, No. 2, pp. 162–181, http://dx.doi.org/10.2138/am-2020-7010

Franz G., Lyckberg P., Khomenko V., Chournousenko V., Schulz H.-M., Mahlstedt N., Wirth R., Glodny J., Gernert U., Nissen J. (2022) Fossilization of Precambrian microfossils in the Volyn pegmatite, Ukraine. *Biogeosciences*, Vol. 19, No. 6, pp. 1795–1811, http://dx.doi.org/10.5194/bg-19-1795-2022

Franz G., Khomenko V., Lyckberg P., Chournousenko V., Struck U., Gernert U., Nissen J. (2023) The Volyn biota (Ukraine) – 1.5 Ga old (micro)fossils in 3D-preservation, a spotlight on the 'boring billion'. *Biogeosciences*, Vol. 20, pp. 1901–1924, http://dx.doi.org/10.5194/egusphere-2022-1116

Ginzburg A.I., Bulgacov V.S., Vasilishin I.S., Luk'yanova V.T., Solntseva L.S., Urmanova A.M., Uspensky V.A. (1987) Kerite from pegmatites of Volyn. *Doklady Akademii Nauk SSSR*, Vol. 292, pp. 188–191 [in Russian].

Gorlenko V.M., Zhmur S.I., Duda V.I., Suzina N.E., Osipov G.A., Dmitriev V.V. (2000) Fine structure of fossilized bacteria in Volyn kerite. *Origin of Life and Evolution of the Biosphere*, Vol. 30, pp. 567–577.

Grundmann G., Giuliani G. (2002) Emeralds of the World. *extraLapis English*, No. 2, pp. 24–35.

Gurskyi D.S., Esypchuk K.Yu., Kalinin V.I. (2006) *Mineral Deposits of Ukraine. Vol. II: Industrial Mineral Deposits*. Centre of Europe Publishing House, Kyiv-Lviv, 552 pp. [in Ukrainian].

Ivanovich P.V., Alekseevich D.S. (2007) *Mineralogy of the Volynian Chamber Pegmatites, Ukraine*. EKOST Association, Moscow, 128 pp.

Kalyuzhnyi V.A., Voznyak D.K., Gigashvili G.M. (1971) *Mineral Forming Fluids and Mineral Paragenesis of Chamber Pegmatites of Ukraine*. Naukova Dumka, Kyiv, 216 pp. [in Ukrainian].

Khomenko V.M., Vyshnevskyi O.A., Gnelytska Z.T., Kamenchuk V.K. (2007) Crystal chemistry of beryl from Volyn deposit on the basis of microprobe analyses, optical and IR spectroscopic data. *Mineralogical Journal (Ukraine)*, Vol. 29, No. 3, pp. 26–38 [in Ukrainian].

Khomenko V.M., Savchuk Ye.O., Vyshnevskyi O.A., Dovbnya N.A. (2010) Influence of irradiation on state of Fe-ions in Volyn beryl. *Proceedings of the Ukrainian Mineralogical Society*, Vol. 7, pp. 64–71.

Koshil I.M., Vasilishin I.S., Pavlishin V.I., Panchenko V.I. (1991) Geologischer Aufbau und Mineralogie der Pegmatite in Wolynien, Ukraine. *Lapis*, Vol. 10, pp. 28–41.

Kurumathoor R., Franz G. (2018) Etch pits on beryl as indicators of dissolution behaviour. *European Journal of Mineralogy*, Vol. 30, No. 1, pp. 107–124, http://dx.doi.org/10.1127/ejm/2018/0030-2703

Lahti S.I., Kinnunen K.A. (1993) A new gem beryl locality: Luumäki, Finland. *G&G*, Vol. 29, No. 1, pp. 30–37, http://dx.doi.org/10.5741/GEMS.29.1.30

Lazarenko E.K., Pavlishin V.I., Latysh V.T., Sorokin Ju G. (1973) Mineralogy and genesis of the chamber pegmatites of Volyn Lvov. *Vysshaja shkola*, 360 pp. [in Russian].

Linnen R.L., Van Lichtervelde M., Černý P. (2012) Granitic pegmatites as sources of strategic metals. *Elements*, Vol. 8, No. 4, pp. 275–280, http://dx.doi.org/10.2113/gselements.8.4.275

London D. (2008) *Pegmatites*. Canadian Mineralogist, Special Publication No. 10, Mineralogical Association of Canada, Québec, 347 pp.

Lukashev A.N. (1976) *Depth of Pegmatite Formation*. Nedra, Moscow, 152 pp. [in Russian].

Lu'kyanova, V.T., Lobzova, R.V., and Popov, V.T. (1992) Filaceous kerite in pegmatites of Volyn. *Izvestiya Ross. Akademii Nauk Ser. Geologicheskaya, 5*, pp. 102–118 [in Russian].

Lyckberg P. (2004) Ein Neufund phantastischer grüner Edelberylle aus Luumäki, Karelien, Finnland. *Mineralien-Welt*, Vol. 6, pp. 38–45 [in German].

——— (2005) Gem beryl from Russia and Ukraine. In *Beryl and Its Color Varieties*. Lapis Intl., East Hampton, Connecticut, pp. 49–57.

Lyckberg P., Chornousenko V., Wilson W.E. (2009) Famous mineral localities: Volodarsk-Volynski, Zhitomir Oblast, Ukraine. *Mineralogical Record*, Vol. 40, pp. 473–506.

Lyckberg P., Chournousenko V., Chournousenko O. (2019) Giant heliodor and topaz pockets of the Volodarsk chamber pegmatites, Korosten pluton, Ukraine. In *Proceedings of the 36th International Gemmological Conference*, Nantes, France, August 27–31, pp. 78–83.

Philpotts A.R., Ague J.J. (2022) *Principles of Igneous and Metamorphic Petrology*, 3rd ed. Cambridge University Press, Cambridge, UK.

Platonov A.N., Taran M.N., Balitsky V.S. (1984) *The Nature of the Color of Gems*. Nedra, Moscow, 196 pp. [in Russian].

Platonov A.N., Khomenko V.M., Taran M.N. (2016) Crystal chemistry, optical spectra and color of beryl. I. Heliodor and golden beryl - two varieties of natural yellow beryl. *Mineralogical Journal (Ukraine)*, Vol. 38, No. 2, pp. 3–14 [in Russian].

Sahama T.G. (1966) Polygonal growth of beryl. *Bulletin of the Geological Society of Finland*, Vol. 222, pp. 31–42.

Schmetzer K., Berdesinski W., Bank H. (1975) Farbveränderungen von Edelsteinen der Beryllgruppe. *Zeitschrift der Deutschen Gemmologischen Gesellschaft*, Vol. 24, No. 2, pp. 81–87.

Shestopalov V., Shybetskyi I., Pochtarenko V., Shymkiv L., Kolaibina I., Shurpach N., Petrenko L., Rudenko Yu., Borysova T. (2020) *Screening of Ukraine for Geological Disposal of Radioactive Waste*. Novyi Druk, Kyiv, 134 pp. [in Ukrainian].

Shumlyanskyy L., Belousova E., Petrenko O. (2017) Geochemistry of zircons from basic rocks of the Korosten anorthosite-mangerite-charnockite-granite complex, north-western region of the Ukrainian Shield. *Mineralogy and Petrology*, Vol. 111, No. 4, pp. 459–466, http://dx.doi.org/10.1007/s00710-017-0514-2

Shumlyanskyy L., Franz G., Glynn S., Mytrokhyn O., Voznyak D., Bilan O. (2021) Geochronology of granites of the western Korosten AMCG complex (Ukrainian Shield): Implications for the emplacement history and origin of miarolitic pegmatites. *European Journal of Mineralogy*, Vol. 33, No. 6, pp. 703–716, http://dx.doi.org/10.5194/ejm-33-703-2021

Simmons W.B. (2014) Gem-bearing pegmatites. In L.A. Groat, Ed., *Geology of Gem Deposits*, Mineralogical Association of Canada, Short Course Series, Vol. 44, pp. 257–304.

Vasylyshyn I.S., Indutny V.V., Pavlyshyn V.I. (2001) Museum of Precious and Decorative Stones. State Gemmological Centre of Ukraine, Kyiv, 100 pp. [in Ukrainian].

Voznyak D.K. (2007) *Microinclusions and Reconstruction of Conditions of Endogenous Mineralogenesis*. Naukova Dumka, Kyiv, 279 pp. [in Ukrainian].

Voznyak D.K., Khomenko V.M., Franz G., Wiedenbeck M. (2012) Physico-chemical conditions of the late stage Volyn pegmatite evolution: Fluid inclusions in beryl studied by thermobarometry and IR-spectroscopy methods. *Mineralogical Journal (Ukraine)*, Vol. 34, pp. 26–38 [in Ukrainian].

Wood D.L., Nassau K. (1968) The characterization of beryl and emerald by visible and infrared absorption spectroscopy. *American Mineralogist*, Vol. 53, No. 5-6, pp. 777–800.

Zhmur S.I. (2003) Origin of Cambrian fibrous kerites of the Volyn region. *Lithology and Mineral Resources*, Vol. 38, pp. 55–73, http://dx.doi.org/10.1023/A:1021827724818